

Supplementary Material

Energy Transfer Induced Blue-Light Excited Broadband Near-infrared

Luminescence in Fluoride $\text{Na}_3\text{AlF}_6:\text{Mn}^{4+},\text{Fe}^{3+}$

Fanquan He^a, Enhai Song^{a*} and Qinyuan Zhang^{a,b*}

^aState Key Laboratory of Luminescent Material and Devices, Guangdong Provincial Key Laboratory of Fiber Laser Materials and Applied Techniques, School of Materials Science and Engineering, South China University of Technology, Guangzhou 510641, China.

^bSchool of Physics and Optoelectronics, South China University of Technology, Guangzhou 510641, China

*Correspondence: msehsong@scut.edu.cn (E. H. Song); qyzhang@scut.edu.cn (Q. Y. Zhang)

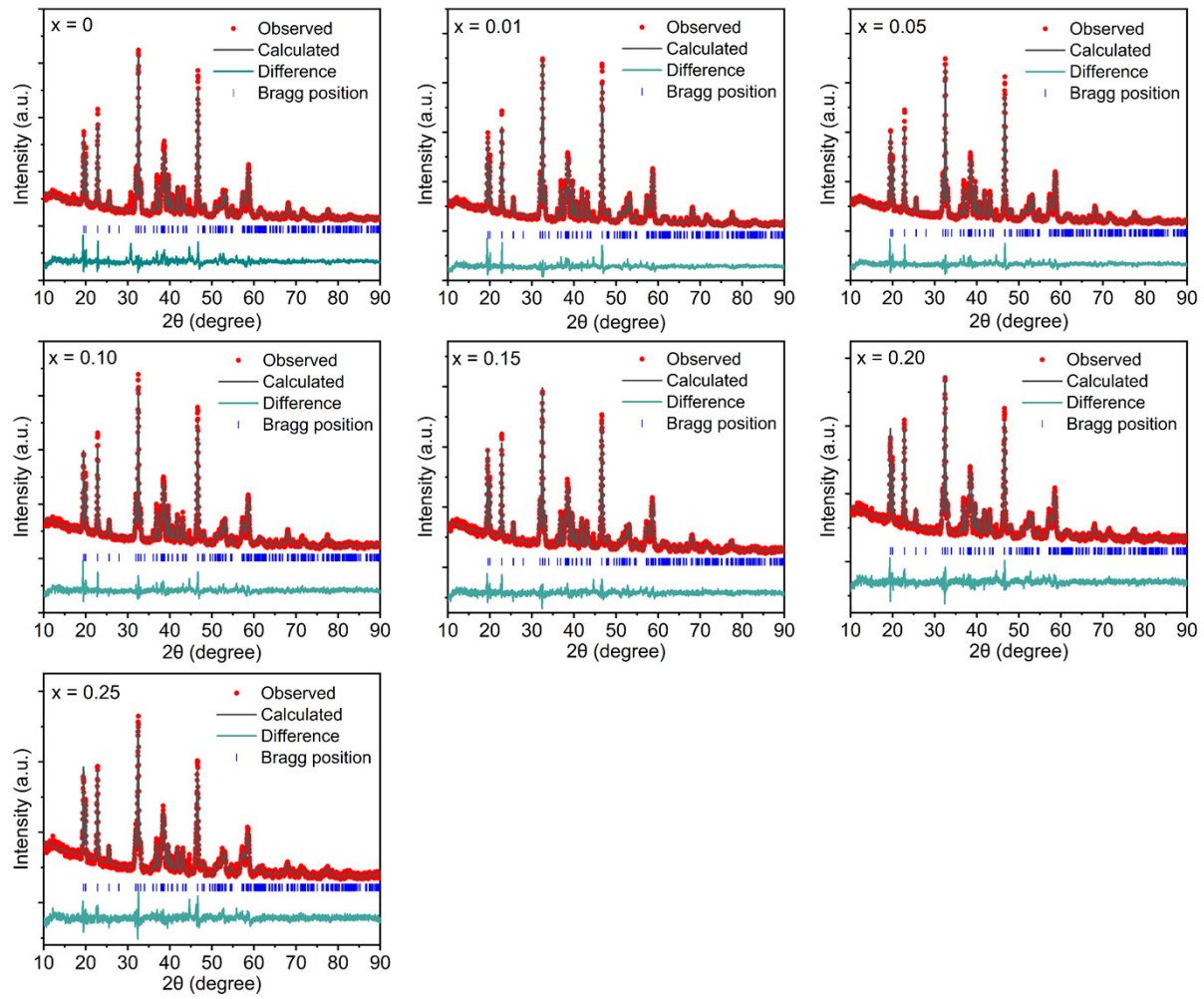


Fig. S1. Rietveld refinement results of NAF:0.03Mn⁴⁺, xFe³⁺ ($x = 0$ -0.25).

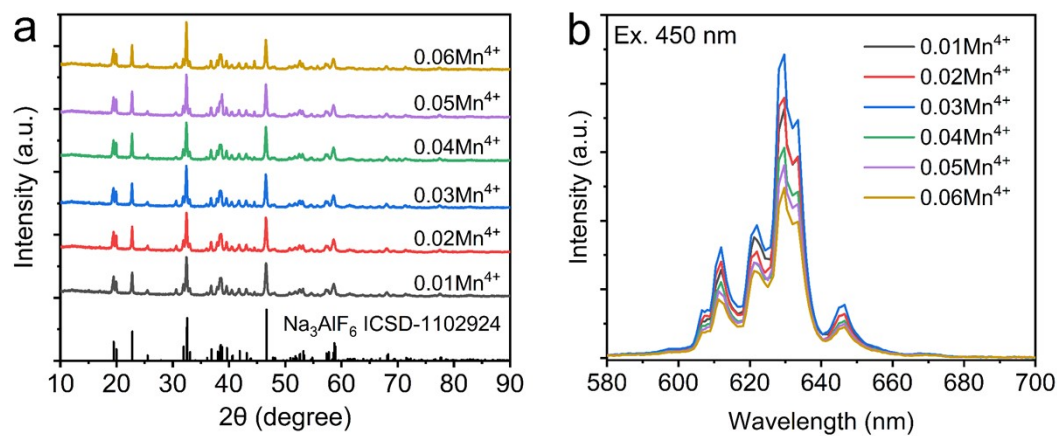


Fig. S2. (a) XRD patterns and (b) emission spectra of Na_3AlF_6 : $y\text{Mn}^{4+}$ ($y = 0.01$ - 0.06).

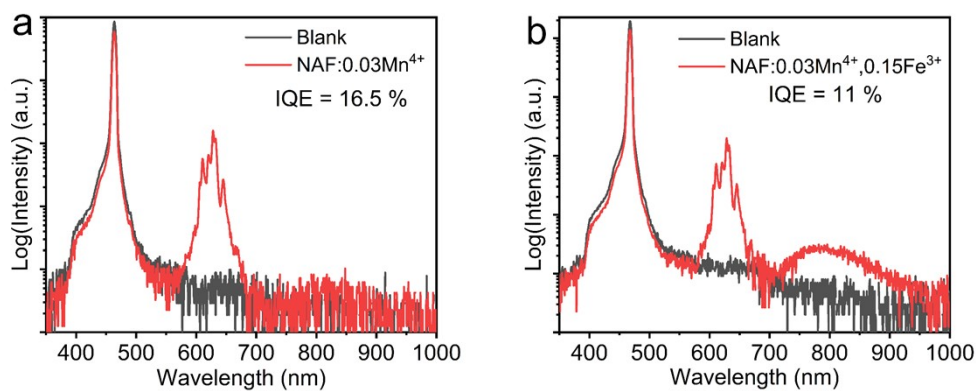


Fig. S3. The quantum efficiency results of NAF:0.03Mn⁴⁺ (a) and NAF:0.03Mn⁴⁺, 0.15Fe³⁺ (b) upon excitation at 463 nm blue light. The internal quantum efficiency (IQE) can be calculated by the following equation:

$$\text{IQE} = \frac{\int L_s}{\int E_B - E_S} \times 100\% \quad (\text{S1})$$

where L_s means the emitted photons of the samples, E_s and E_B is the integrated area of the excitation light with and without the phosphor.

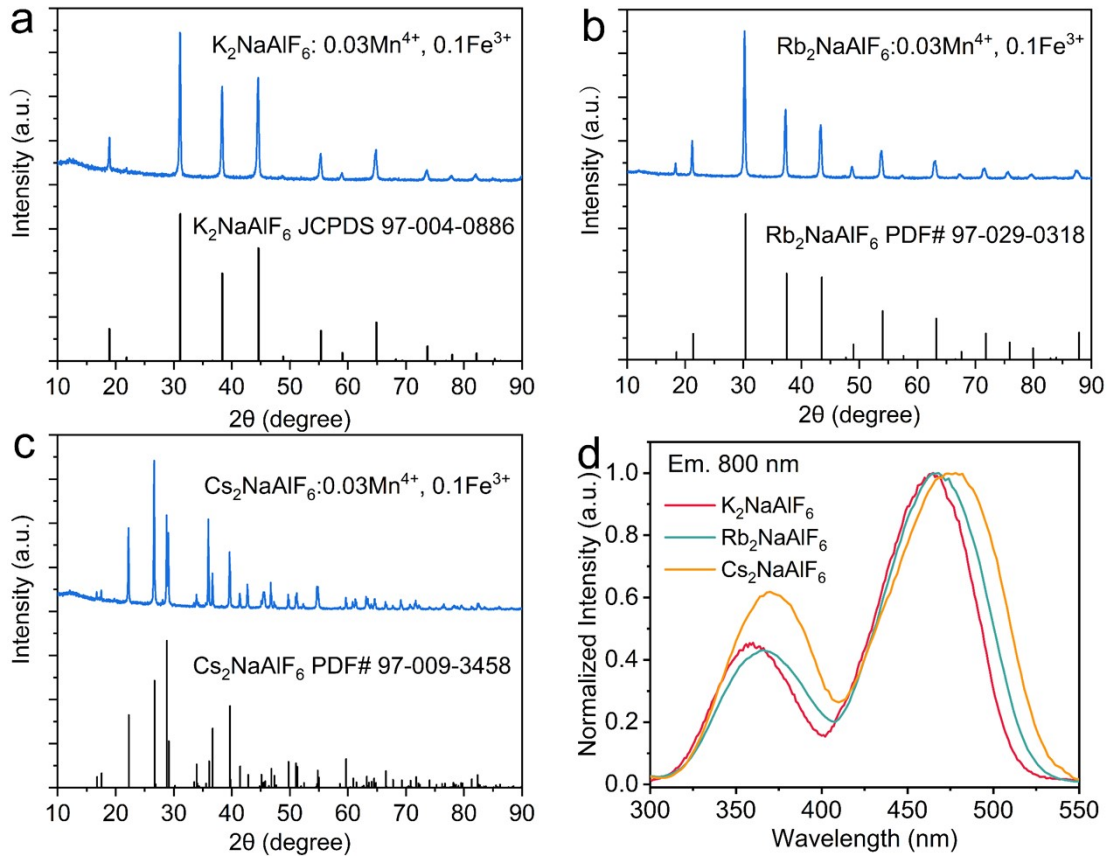


Fig. S4. (a-c) XRD patterns of K_2NaAlF_6 : $0.03\text{Mn}^{4+}, 0.1\text{Fe}^{3+}$, $\text{Rb}_2\text{NaAlF}_6$: $0.03\text{Mn}^{4+}, 0.1\text{Fe}^{3+}$, $\text{Cs}_2\text{NaAlF}_6$: $0.03\text{Mn}^{4+}, 0.1\text{Fe}^{3+}$. (b) The normalized excitation spectra of K_2NaAlF_6 : $0.03\text{Mn}^{4+}, 0.1\text{Fe}^{3+}$, $\text{Rb}_2\text{NaAlF}_6$: $0.03\text{Mn}^{4+}, 0.1\text{Fe}^{3+}$, $\text{Cs}_2\text{NaAlF}_6$: $0.03\text{Mn}^{4+}, 0.1\text{Fe}^{3+}$.

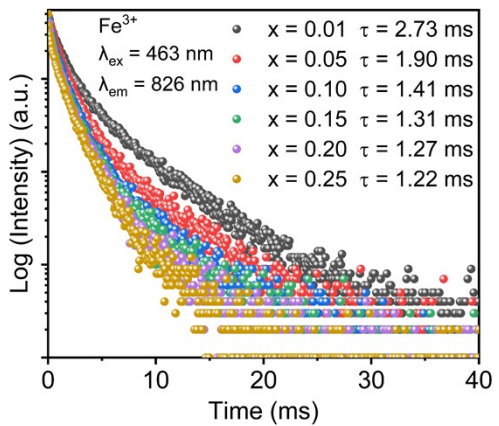


Fig. S5. The decay curves of NAF:0.03Mn⁴⁺, xFe³⁺ monitored at 826 nm. The continuous decrease lifetime with increasing Fe³⁺ concentration can be understood since concentration quenching of Fe³⁺ will result in increased non-radiative transition probability and thus the decay became faster.

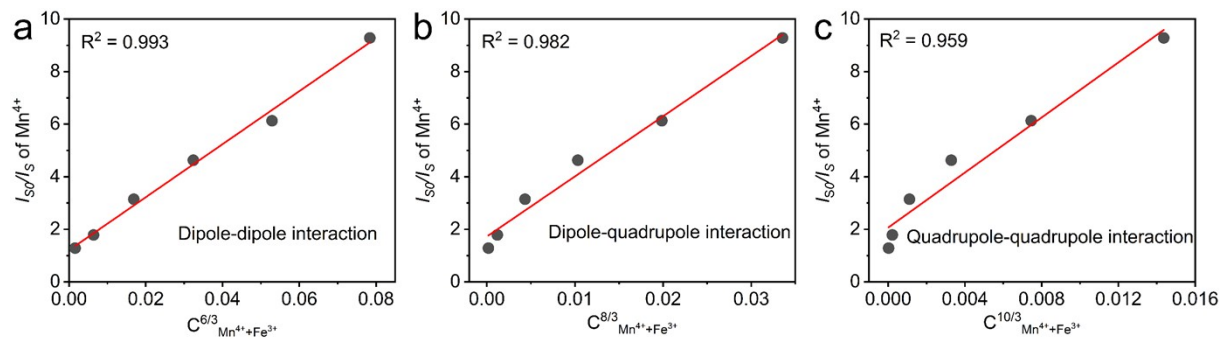


Fig. S6. $I_{S0}/I_S - C^{\alpha/3}$ diagram of NAF:0.03Mn⁴⁺, xFe³⁺.

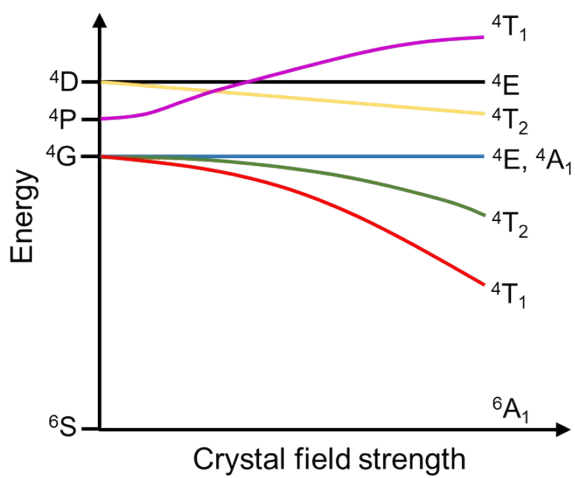


Fig. S7. The Tanabe–Sugano diagram for Fe^{3+} in an octahedral site.

Table S1. Main cell parameters of processing and refinement of the $\text{Na}_3\text{AlF}_6:0.03\text{Mn}^{4+}, \text{xFe}^{3+}$ samples.

x (Fe^{3+})	Space group	Cell Parameters				$\text{R}_p, \text{R}_{wp} (\%), \chi^2$
		a (Å)	b (Å)	c (Å)	V (Å ³)	
0	P2 ₁ /c	5.4085	5.5988	9.46200	235.609	7.86, 10, 3.89
0.01	P2 ₁ /c	5.4099	5.5991	9.4617	235.663	7.05, 9.34, 3.09
0.05	P2 ₁ /c	5.4115	5.6021	9.4655	235.964	6.30, 8.32, 2.69
0.10	P2 ₁ /c	5.4166	5.6084	9.4748	236.711	5.99, 7.95, 2.65
0.15	P2 ₁ /c	5.4181	5.6108	9.4763	236.939	5.17, 6.68, 2.11
0.20	P2 ₁ /c	5.4202	5.6131	9.4801	237.241	5.16, 6.64, 2.17
0.25	P2 ₁ /c	5.4223	5.6159	9.4844	237.544	4.94, 6.35, 2.24

Table S2. Fractional atomic coordinates and Wyckoff sites of the Na₃AlF₆:0.03Mn⁴⁺, 0.15Fe³⁺ sample.

Atoms	x	y	z	Wyckoff sites	Occ.
Na1	0.27186	0.05423	0.75375	4e	1
Na2	0.5	0	0.5	2d	1
Al1	0	0	0	2a	0.82
Mn1	0	0	0	2a	0.03
Fe1	0	0	0	2a	0.15
F1	0.11350	0.04448	0.21906	4e	1
F2	0.22960	0.73172	0.06265	4e	1
F3	0.32695	0.17715	0.04772	4e	1

Table S3. The excitation peak wavelength (λ_{ex}), emission peak wavelength (λ_{em}) and FWHM values of Fe³⁺-doped phosphors.

Phosphors	λ_{ex} (nm)	λ_{em} (nm)	FWHM (nm)	Ref.
KAl ₁₁ O ₁₇ :Fe ³⁺	340	770	-	¹
Ca ₂ InSbO ₆ :Fe ³⁺	340	935	126	²
Ca ₂ LuSbO ₆ :Fe ³⁺	336	927	128	³
Ca ₂ YSbO ₆ :Fe ³⁺	345	938	135	
SrAl ₁₂ O ₁₉ : Fe ³⁺	270	812	-	⁴
CaAl ₁₂ O ₁₉ :Fe ³⁺	260	810	-	⁵
LiAl ₅ O ₈ :Fe ³⁺	284	673	-	⁶
NaAl ₅ O ₈ :Fe ³⁺	346	754	-	⁷
NaScSi ₂ O ₆ :Fe ³⁺	300	900	135	⁸
Sr ₉ Ga(PO ₄) ₇ :Fe ³⁺	330	915	155	⁹
ZnGa ₂ O ₄ :Fe ³⁺	344	720	70	¹⁰
BaSnO ₃ :Fe ³⁺	380	896	105	¹¹
NAF:Mn ⁴⁺ , Fe ³⁺	463	826	127	This work

References

1. G. Liu, S. Zhang and Z. Xia, *Opt. Lett.*, 2023, **48**, 1296-1299.
2. D. Liu, G. Li, P. Dang, Q. Zhang, Y. Wei, L. Qiu, M. S. Molokeev, H. Lian, M. Shang and J. Lin, *Light Sci. Appl.*, 2022, **11**, 1296.
3. X. He, Y. Chen, C. Xia, K. Muhammad, Z. D. Syeda, Y. Guo, S. Xie, X. Liu and L. Li, *J. Amer. Ceram. Soc.*, 2024, **107**, 1-13.
4. S. Zhang, J. Zeng, H. Ye, Z. Li, Y. Lv, L. Xiong, Y. Hu and Y. Li, *Adv. Photon. Res.*, 2023, **4**, 2300011.
5. P. Rodionovs, M. Kemere, A. Antuzevics, A. Sarakovskis, A. Fedotovs and U. Rogulis, *Opt. Mater.*, 2023, **144**, 114342.
6. Y. Yin, X. Zhang, L. Guangxi and W. Haibo, *Chin. J. Lumin.*, 2010, **31**, 473-476.
7. K. Cheng, W. Huang, X. Liu, X. Gong and C. Deng, *J. Alloys Comp.*, 2023, **964**, 171240.
8. X. Zhang, D. Chen, X. Chen, C. Zhou, P. Chen, Q. Pang and L. Zhou, *Dalton Trans.*, 2022, **51**, 14243-14249.
9. F. Zhao, Y. Shao, Z. Song and Q. Liu, *Inorg. Chem. Front.*, 2023, **10**, 6701-6710.
10. L. Xiang, X. Zhou, Y. Wang, L. Li, S. Jiang, G. Xiang, C. Jing, J. Li and L. Yao, *J. Lumin.*, 2022, **252**, 119293.
11. M. Li, Y. Jin, H. Wu and Y. Hu, *Mater. Res. Appl.*, 2023, **17**, 286-294.